Transition metal compounds with S/N-functionalized NHC ligands: structures, redox properties and electrocatalytic activity

Luo, S.; Luo S.

CHAPTER 5

Nickel Compounds of Pyridine-Amide-Functionalized Carbene Ligands: Synthesis, Structure and Electrocatalytic Activity

*Two pyridyl-amide substituted (benz)imidazolium salts H_2**L1**Cl and H_2**L2**Cl were synthesized and successfully employed as ligand precursors for the syntheses of novel nickel(II) complexes [Ni(**L1**)]Cl and [Ni(**L2**)]PF_6 bearing tetradentate ligands including an N-heterocyclic carbene (NHC) functionality. Single crystal X-ray crystallography revealed that the nickel ions in both compounds are in slightly distorted square-planar geometries. Cyclic voltammetry of the two compounds showed irreversible reduction events. In the solvent dimethylformamide in presence of acetic acid, the imidazolidene-based complex [Ni(**L1**)]Cl shows higher catalytic activity in the electrocatalytic proton reduction than the nickel compound of the benzimidazolidene-based ligand. Moreover, the water-soluble complex [Ni(**L1**)]Cl appeared to be an active electrocatalyst for proton reduction in aqueous buffer solutions at pH 6.8. The stability of this complex in aqueous solutions is low.*

This chapter will be published. S. Luo, M.A. Siegler, and E. Bouwman, manuscript in preparation.

5.1 Introduction

Dihydrogen gas is a promising energy carrier and has emerged as a good alternative for fossil fuel resources, which can meet the rapidly increasing global energy demands.[1] Aiming to avoid the use of the expensive Pt-based catalyst, the study of the hydrogen evolution reaction (HER) using molecular catalysts based on non-noble metals has received extensive attention in recent decades. The development of an inexpensive catalyst with high catalytic turnover rates is the ultimate goal. However, a high stability and low overpotential of the catalyst are also of great significance. Hydrogenase enzymes act as effective catalysts in the hydrogen evolution reaction at ambient temperatures and pressures. But most of the hydrogenase enzymes only work in anaerobic conditions and suffer from oxidative deactivation.[2] On the other hand, synthetic molecular catalyst often suffer from decomposition in aqueous acidic media, resulting in the formation of heterogeneous catalyst systems.[3]

In the last decade the cobaloxime-type catalysts[4] and nickel-based catalysts with diphosphane ligands[5] have proven to have high activity in the electrocatalytic proton reduction reaction. Meanwhile, other molecular catalyst based on molybdenum,[6] zinc,[7] manganese,[8] and copper[9] have been reported to have outstanding activities. Our interest is in the development of novel nickel-based homogeneous catalysts supported by N-heterocyclic carbene (NHC) ligands.[10, 11] Such NHC ligands functionalized with pyridine groups have been used to synthesize nickel and palladium complexes that were found to be efficient catalysts for the Kumada cross-coupling[10-12] and Heck-type coupling reactions.[13] Nevertheless, so far metal-NHC complexes have received little attention regarding their potential electrochemical properties and activity in electrocatalysis.[14, 15] Herein, we report the synthesis and characterization of two novel nickel compounds supported by tetradentate N-functionalized carbene ligands. We report their redox properties in the solvent dimethylformamide as well as their electrocatalytic activity for proton reduction in weakly acidic aqueous conditions.

5.2 Results and Discussion

5.2.1 Synthesis of ligand precursors and the Ni-NHC complexes

The two new (benz)imidazolium salts H_2**L1**Cl and H_2**L2**Cl were designed for their use as ligand precursors for the formation of tetradentate anionic NHC ligands, comprising amide and pyridine donor moieties. Alkylation of N-pyridylmethyl(benz)imidazole didn't appeared to be straightforward. The relatively high reactivity of the pendant pyridyl group resulted in the formation of oligomeric side products (Figure 5.1), giving relatively low yields of the desired products (30%-50%). The (benz)imidazolium salts were characterized by NMR spectroscopy and electrospray ionization mass spectrometry (ESI-MS). In the ^{1}H NMR spectra the characteristic downfield signals for the imidazolium NCHN and amide NH protons were observed at 9.32 and 9.15 ppm for H_2**L1**Cl and at 10.02 and 9.44 ppm for

H_2**L2**Cl. The ESI-MS exhibited base peaks corresponding to the $[M - Cl]^+$ (benz)imidazolium cations.

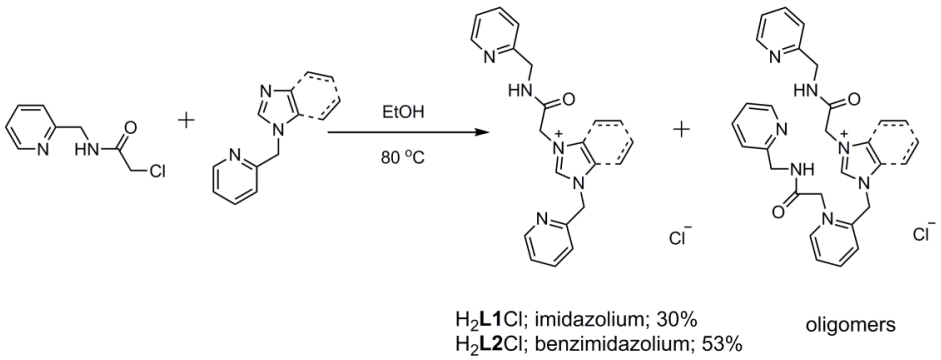

*Figure 5.1. Synthetic route of the ligand precursors H_2**L1**Cl and H_2**L2**Cl.*

Nickel(II) complexes were prepared by reacting the ligand precursors H_2**L1**Cl and H_2**L2**Cl with Ni(dme)Cl_2 in DMF in the presence of K_2CO_3 at room temperature and were isolated as yellow solids. The complex [Ni(**L1**)]Cl was obtained as a pure product after dilution of the reaction mixture with water and an extraction with dichloromethane (DCM). Unfortunately, this purification method did not work for the benzimidazole-based compound [Ni(**L2**)]Cl. Therefore, by addition of NH_4PF_6 the chloride anion was replaced with the hexafluoridophosphate counter ion. The crystalline yellow needle-shaped crystals of [Ni(**L2**)]PF_6 were obtained directly from the filtrate after the reaction. The absence in the ^{1}H NMR spectra of the nickel compounds of the characteristic downfield signals for the amide NH and imidazolium NCHN protons indicates the successful creation of the deprotonated amide and carbene moieties and their coordination to the nickel(II) center. The ESI-MS spectra exhibit base peaks corresponding to the $[M - Cl]^+$ or $[M - PF_6]^+$ cationic complexes. Recrystallized samples of the nickel compounds were dried in vacuo before elemental analyses were performed; however, the analysis result still showed the presence of small amounts of H_2O. Compound [Ni(**L1**)]Cl readily dissolves in water, whereas compound [Ni(**L2**)]PF_6 is soluble in DMF but hardly dissolves in water.

5.2.2 Structural characterization of Ni-NHC complexes

Single crystals of [Ni(**L1**)]Cl suitable for X-ray structure determination were obtained by vapor diffusion of diethyl ether into an acetonitrile solution of the complex. Single crystals of [Ni(**L2**)]PF_6 were picked from the yellow needle-like crystals that were obtained directly from the reaction mixture. Projections of the cationic complexes are shown in Figure 5.2. The crystallographic and refinement data are provided in Table AV.1, and selected bonds lengths and angles are given in Table AV.2. The imidazole-based compound [Ni(**L1**)]Cl crystallized in the space group $P2_1/c$. Apart from the cationic complex and the non-coordinating chloride anion the asymmetric unit contains three lattice water molecules. The

benzimidazole-based compound [Ni(**L2**)]PF_6 crystallized in the triclinic space group P$\bar{1}$, with one cationic complex and one PF_6 anion in the asymmetric unit.

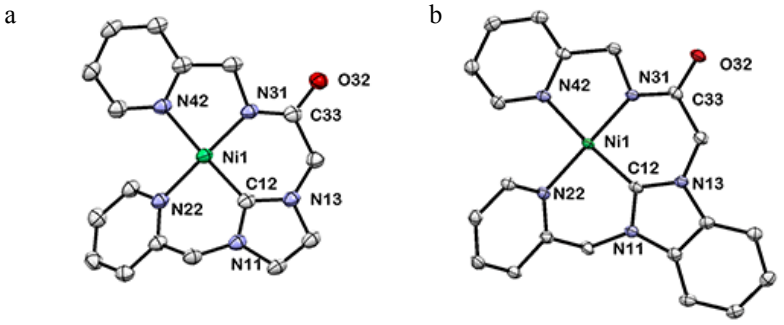

*Figure 5.2. Displacement ellipsoid plots (50% probability level) of the cations of compounds [Ni(**L1**)]Cl (a) and [Ni(**L2**)]PF_6 (b) at 110(2) K. Hydrogen atoms, counter ions and the lattice solvents are omitted for clarity.*

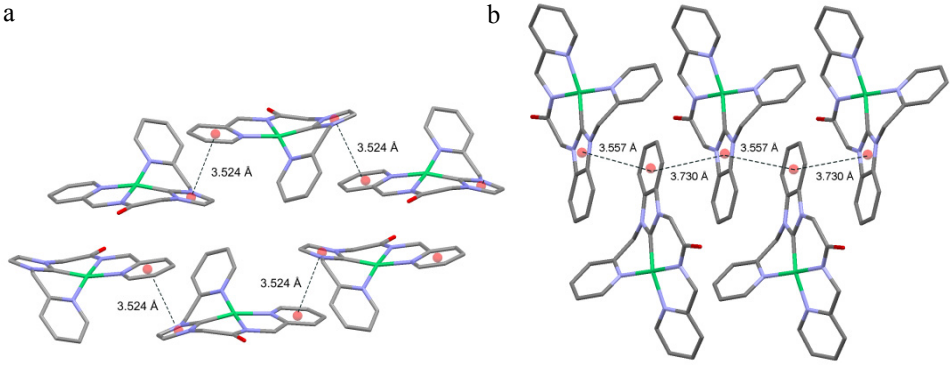

*Figure 5.3. View of π-stacking interactions in [Ni(**L1**)]Cl (a) and [Ni(**L2**)]PF_6 (b). Distances given are between ring centers.*

In both structures the nickel(II) ion is in a four-coordinate [$NiCN_3$] chromophore with short Ni–C (carbene) and Ni–N (amide) bonds, and two longer Ni–N (pyridine) bond distances. The nickel ions are in slightly distorted square-planar geometries (τ_4 = 0.178 for [Ni(**L1**)]Cl and τ_4 = 0.177 for [Ni(**L2**)]PF_6).[16] The Ni–N_{amide} bond in both complexes (1.873(3) Å and 1.856(2) Å, respectively) is slightly longer than in other reported nickel compounds with pyridylmethyl-amide groups (ranging from 1.81 to 1.85 Å).[17-19] The carbonyl C33–O32 bond in compound [Ni(**L1**)]Cl is slightly longer than the one in compound [Ni(**L2**)]PF_6, probably due to the presence of hydrogen bonds between the carbonyl O32 and lattice water molecules in [Ni(**L1**)]Cl. The structure [Ni(**L1**)]Cl is further stabilized by intermolecular π-π stacking interactions between pyridine and carbene rings with a distance of 3.524 Å. The chloride ion is at a distance of 3.443 Å of the nickel center.

Intermolecular π-π stacking interactions in the structure of [Ni(**L2**)]PF_6 occur between adjacent benzimidazole rings with distances of 3.525 and 3.677 Å (Figure 5.3).

5.2.2 Electrochemical studies in dimethylformamide

The redox properties of the two compounds were investigated with cyclic voltammetry in dry DMF solutions containing 0.1 M tetrabutylammonium hexafluoridophosphate (TBAP) as the supporting electrolyte, under a stream of argon. For the imidazole-based complex [Ni(**L1**)]Cl an irreversible reduction was found at −1.4 V vs. Ag/AgCl; in the anodic return scan one irreversible oxidative peak was found at −0.84 V (Figure AV.1.1). The benzimidazole-based complex [Ni(**L2**)]PF_6 showed the first irreversible reduction to occur at −1.27 V vs. Ag/AgCl. The less negative reductive potential of [Ni(**L2**)]PF_6 must be due to the benzimidazole-based carbene being a more electron-withdrawing group, which makes the nickel center relatively electron poor. The oxidative peak **c** in the return scan of [Ni(**L2**)]PF_6 is also located at a less negative potential at −0.75 V. Upon expanding the scan window down to −2.2 V, a second irreversible reductive peak is found at −2.02 V and three small oxidative waves **c**, **d** and **e** appeared at −0.75, −0.64 and −0.26 V, respectively (Figure 5.4). It indicate that the new oxidative processes **d** and **e** are related to the second reductive event **b**. Both complexes [Ni(**L1**)]Cl and [Ni(**L2**)]PF_6 show irreversible redox nature, indicating that electron transfer is immediately followed by a fast chemical reaction or structural rearrangement.[20]

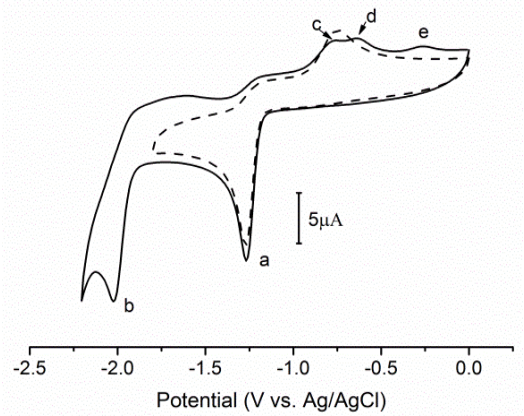

*Figure 5.4. Cyclic voltammograms of [Ni(**L2**)]PF_6 (1 mM) recorded in DMF containing 0.1 M TBAP as supporting electrolyte in different scan windows (dashed line = 0 to −1.8 V; solid line = 0 to −2.2 V) at scan rate 0.1 V/s, using a glassy carbon working electrode.*

The electrocatalytic activity of the two compounds for HER were studied in DMF solutions, using acetic acid as proton source. For compound [Ni(**L1**)]Cl a catalytic reductive current response appeared with an onset potential at −1.53 V in presence of 10 mM acid (Figure 5.5a). For compound [Ni(**L2**)]PF_6 a similar catalytic reductive current was observed with an onset potential of −1.69 V. However, before the catalytic wave of [Ni(**L2**)]PF_6 one small additional irreversible reduction appeared at −1.60 V (Figure 5.5b). With increasing acid

concentration this additional peak becomes invisible, as it overlaps with the following large catalytic peak (Figure AV.2).

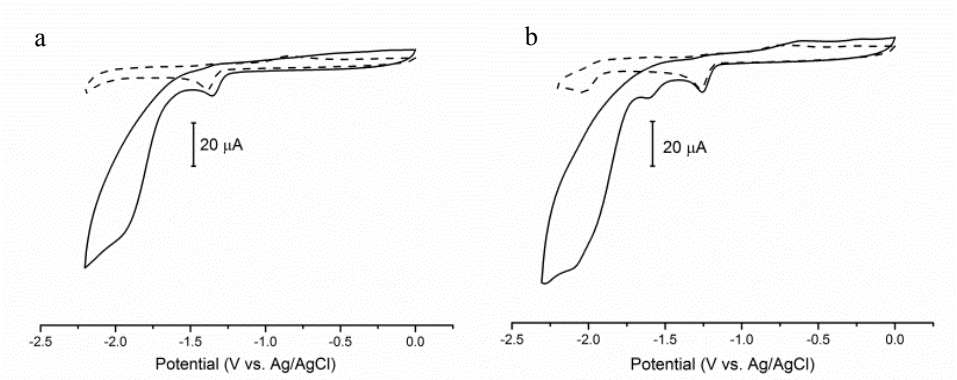

*Figure 5.5. Cyclic voltammograms of (a) 1 mM of [Ni(**L1**)]Cl and (b) 1 mM of [Ni(**L2**)]PF_6 recorded in DMF containing 0.1 M TBAP as supporting electrolyte at scan rate 0.1V/s in absence (dashed line) and in presence (solid line) of 10 mM acetic acid, using glassy carbon working electrode.*

In general, for an irreversible catalytic reaction following a reversible charge transfer (P + $e^- \rightleftharpoons$ Q; Q + A $\xrightarrow{k}$ P+B), the k_{obs} can be deduced from i_c.

$$i_c = n'FAC_P^0\sqrt{Dk_{obs}} \qquad (1)$$

If equation (1) is combined with the Randles-Sevcik equation (2), the relationship (3) is obtained.

$$i_p = 0.4463n'FAC_P^0\left(\frac{n\prime FvD}{RT}\right)^{1/2} \qquad (2)$$

$$\frac{i_c}{i_p} = \frac{1}{0.4463}\sqrt{\frac{RTk_{obs}}{n\prime Fv}} \qquad (3)$$

$$k_{obs} = kC_A^0 \qquad (4)$$

Where i_c is the maximum current of the catalytic peak, and i_p is the plateau current of the non-catalytic reduction wave, *n'* is the number of electrons transferred to P from the electrode, F is Faraday's constant, *A* is the area of the electrode, C_P^0 is the catalyst concentration, C_A^0 is the substrate concentration, *D* is the diffusion coefficient, *k* is the rate constant.

When specialized the reaction to the two electron transferred hydrogen evolution reaction (HER), the order of the reaction with respect to acid can be identified using the following equations:[21-23]

$$k_{obs} = k[H^+]^x \qquad (5)$$

$$\frac{i_c}{i_p} = \frac{n}{0.4463}\sqrt{\frac{RTk[\mathrm{H}^+]^x}{Fv}} \qquad (6)$$

Where x is the order of the reaction with respect to protons. n is the number of electrons involved in HER (n = 2).

According to equations (5) and (6), if a plot of i_c/i_p versus the square root of the proton concentration gives a linear correlation, a catalytic reaction has a first-order dependence on proton concentration. Many publications have cited this method to calculate k_{obs} and k for electrocatalytic reactions.[9, 22, 24-27]

Plots of i_c/i_p versus the square root of the acid concentration for the complexes [Ni(**L1**)]Cl and [Ni(**L2**)]PF_6 show a non-linear relationship (Figure AV.3). Instead, plots of i_c/i_p versus acid concentration do show a linear relationship (see Figure 5.6). This relationship reveals that two protons are involved in the rate-determining step of the reaction. Unfortunately, due to the irreversible redox property of both compounds, equation (6) is not suitable for k_{obs} determination for both complexes.[21, 23]

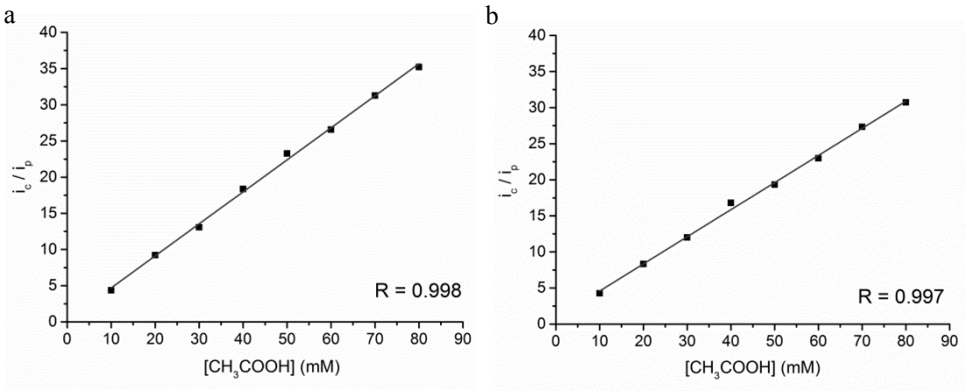

*Figure 5.6. Plot of i_c/i_p vs. [CH_3COOH] (mM) for [Ni(**L1**)]Cl (a) and [Ni(**L2**)]PF_6 (b) in presence of various acid concentration in DMF containing 0.1 M TBAP as supporting electrode at 0.1 V/s, using a glassy carbon working electrode.*

In the presence of 80 mM acetic acid the value of i_c/i_p reaches 35.2 and 30.7 for complex [Ni(**L1**)]Cl and [Ni(**L2**)]PF_6, respectively, indicating that the imidazole-based compound [Ni(**L1**)]Cl is the faster HER catalyst of the two. This difference in activity was confirmed with controlled-potential electrolysis (CPE) experiments (see below). The overpotential for proton reduction in our conditions is 860 mV for [Ni(**L1**)]Cl and 940 mV for [Ni(**L2**)]PF_6, taking homoconjugation of the acid into account.[28] In general, a more electron-donating group such as imidazolylidene will make the metal centre of complex more difficult to reduce, which might increase the overpotential in electrocatalysis. The cyclic voltammogrammes indeed show the reductive events of [Ni(**L1**)]Cl to occur at more

negative potentials compared to those of [Ni(**L2**)]PF_6. Surprisingly, the overpotential for proton reduction is lower for the imidazole-based compound.

Hydrogen production was further confirmed using gas chromatography (GC) monitoring the controlled-potential electrolysis at −1.8 V; the faradaic efficiencies were determined to be around 85% for both [Ni(**L1**)]Cl and [Ni(**L2**)]PF_6. After subtracting the results of a blank reaction (volume of H_2 produced at this potential in absence of catalyst, for data treatment see Appendix I), 185 µL and 105 µL H_2 were generated over 2 h electrolysis in presence [Ni(**L1**)]Cl and [Ni(**L2**)]PF_6, respectively, corresponding to a mere 1.5 and 0.9 mol H_2 per mol of catalyst. The better electrocatalytic activity of [Ni(**L1**)]Cl may tentatively be ascribed to the better electron-donating properties of the imidazole-based carbene, which might facilitate the formation of a metal hydride intermediate.

Thus, the imidazole-based compound [Ni(**L1**)]Cl not only shows higher activity in catalyzing HER, but is also active at a lower overpotential. This anti-correlation indicates that a proton delivery between the ligand and the metal center is operative, which breaks the correlation between energy costs and kinetic barriers.[29]

5.2.3 Electrochemical studies in aqueous solution

As the compound [Ni(**L1**)]Cl shows good solubility in water, the electrochemical properties of [Ni(**L1**)]Cl in aqueous solutions were also investigated. Voltammograms of [Ni(**L1**)]Cl in an 0.2 mM phosphate buffer solution (pH = 6.86) are shown in Figure 5.7a. Compared with the buffer solution without nickel complex, a small irreversible reductive process at −1.36 V is observed, which is followed by a large catalytic current at −1.82 V, which can be assign to HER process. The catalytic current increased with increasing of the scan rate (0.05 to 2 V/s), as shown in Figure 5.7b. At lower scan rate range, the catalytic current increases linearly; when scan rate reach ≥ 0.5 V/s, the current shows a saturated trend (Figure 5.7c).

It was observed that the bright yellow aqueous solution containing [Ni(**L1**)]Cl gradually faded to pale yellow during the electrochemical experiments. In order to investigate whether this color change is related to electrolysis or the stability of the compound in mildly acidic aqueous solutions, ^{1}H NMR spectra were recorded of [Ni(**L1**)]Cl in presence and absence of acid in deuterium oxide. The ^{1}H NMR spectra of a solution of [Ni(**L1**)]Cl in deuterium oxide did not change significantly over a period of more than four days. However, upon addition of an excess of acetic acid-*d*4 the color of the solution visibly faded within 1 hour, and the solution was colorless after one day. The ^{1}H-NMR spectra revealed that nearly 50% of the compound decomposed within 1 h (Figure AV.4). The composition of the colorless solution was investigated with ESI-MS (Figure AV.5). The MS peak located at m/z 309.3 can be assigned to the ligand precursor [HD**L1**]$^+$. Although we investigated the stability of compounds in organic solvent in presence of acid (see Figure AV.6), it appears that the presence of even a weak acid in aqueous solution is

sufficient to cause dissociation of the ligand from the nickel center by protonation of the amidate nitrogen and the carbene carbon atoms.

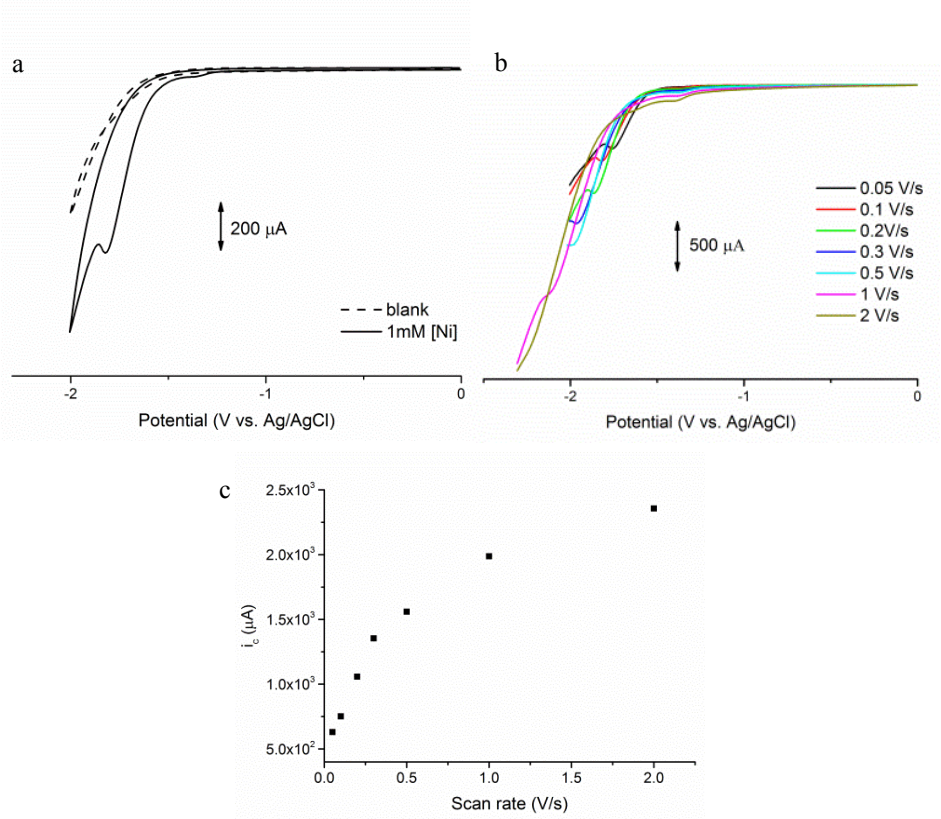

Figure 5.7. (a) *CVs of compound [Ni(**L1**)]Cl recorded in pH = 6.86 phosphate buffer solution (0.2 M) in absence (dashed line) and in presence (solid line) at a scan rate of 0.1 V/s; (b) Forward scans of 1 mM [Ni(**L1**)]Cl in phosphate buffer solution (0.2 M, pH = 6.86) at various scan rates from 0.05 to 2 V/s; (c) plots of catalytic current* vs. scan rate for compound *[Ni(**L1**)]Cl in phosphate buffer solution (0.2 M, pH = 6.86), using glassy carbon as the working electrode. For Ag/AgCl (3 M KCl) reference electrode, E^o = 0.223 V vs. NHE.*

5.3 Conclusion

The two new nickel(II) complexes [Ni(**L1**)]Cl and [Ni(**L2**)]PF_6 bearing pyridyl-amidate substituted tetradentate ligands based on N-heterocyclic carbenes, were isolated and characterized. X-ray structure analysis revealed that the nickel ions in both compounds are in slightly distorted square-planar geometries. Cyclic voltammetry of the two compounds showed irreversible redox events. In dimethylformamide in presence of acetic acid both complexes showed activity for the electrocatalytic reduction of protons into H_2 gas as confirmed by GC quantification. The imidazole-based complex [Ni(**L1**)]Cl shows slightly higher catalytic activity at lower overpotentials compared to the benzimidazole-based compound. Moreover, the water-soluble complex [Ni(**L1**)]Cl appears to be an active

electrocatalyst also in aqueous buffer solutions. Although the compounds appeared to be stable in acidic organic solution, the complex [Ni(**L1**)]Cl is not stable in acidic aqueous solution. Unfortunately, the activity of the compounds for proton reduction appeared to be low, and far from comparable with the well-developed cobaloxime-type and nickel-diphosphane type catalysts. If possible, the catalytic mechanism as well as rate-determining steps need to be identified and studied in priority. Further research needs to focus on finding an explanation for the low catalytic activity of the catalysts based on carbene-type ligands.

5.4 Experimental

5.4.1 Materials

Commercial chemicals were used without further purification. Acetonitrile, tetrahydrofuran, dichloromethane and diethyl ether were obtained from a PureSolv MD5 solvent dispenser. Dry ethanol and dimethylformamide were prepared by adding molecular sieves into commercial anhydrous solvent. The rest commercial solvents were used without further purification. All air-sensitive reactions were performed under argon or dinitrogen gas using standard Schlenk techniques unless mentioned otherwise. The compounds dichlorido(dimethoxyethane)nickel ([Ni(dme)Cl_2]),[30] 2-chloro-N-(pyridin-2-ylmethyl)acetamide,[31] and *N*-pyridin-2-ylmethyl(benz)imidazole[32] were prepared following published procedures.

5.4.2 Analytical methods

^{1}H and ^{13}C spectra were recorded on Bruker 300DPX /400DPX-liq spectrometer. Mass spectra were obtained using a Finnigan Aqueous Mass Spectrometer (MS) with electrospray ionization (ESI). Elemental analyses were performed by the Mikroanalytisches Laboratorium Kolbe, Germany. Cyclic voltammetry was recorded with an Autolab PGstat10 potentiostat controlled by GPES4 software under argon. A 3 mm diameter glassy carbon electrode was used as working electrode and plantium as the counter electrode. The experimental reference electrode was a commercially available Ag/AgCl electrode (E^o = 0.223 V vs. NHE). Ferrocene was added at the end of each measurement as an internal standard when experiments were carried out in organic solvents. Under the used conditions the redox couple of ferrocene was located at $E_{1/2}$ = 0.52 V vs Ag/AgCl with ΔE = 90 ~ 110 mV.

Controlled-potential electrolysis (CPE) experiments were carried out in an H-shaped double-compartment cell. A glassy carbon electrode with a surface area of 0.07 cm^2 was used as the working electrode for electrolysis. As the auxiliary electrode a platinum gauze electrode was used. The reference electrode was a commercially available aqueous Ag/AgCl electrode. The solution containing the sample was bubbled with helium gas for 10 min before measurement and the electrolysis was carried out under an atmosphere of helium. The solutions in both compartments were constantly stirred during electrolysis

experiments. The evolved H_2 gas produced during electrolysis measurements was quantified using gas chromatography, which was performed on a Shimadzu GC2010 at 35ºC fitted with a Supelco Carboxen 1010 molecular sieve column. Two separate experiments were done and the results of two experiments were averaged.

5.4.3 Single crystal x-ray crystallography

All reflection intensities were measured at 110(2) K using a SuperNova diffractometer (equipped with Atlas detector) with Cu *K*α radiation (λ = 1.54178 Å) under the program CrysAlisPro (Version 1.171.37.35 Agilent Technologies, 2014). The same program was used to refine the cell dimensions and for data reduction. The structure was solved with the program SHELXS-2014/7 and was refined on F^2 with SHELXL-2014/7.[33] Analytical numeric absorption correction using a multifaceted crystal model was applied using CrysAlisPro. The temperature of the data collection was controlled using the system Cryojet (manufactured by Oxford Instruments). The H atoms were placed at calculated positions (unless otherwise specified) using the instructions AFIX 23, AFIX 43 with isotropic displacement parameters having values 1.2 *U*eq of the attached C atoms.

Additional notes for the structures:
Compound [Ni(**L1**)]Cl*:* The structure is mostly ordered. The asymmetric contains three lattice water solvent molecules. Two are disordered over two orientations, and the occupancy factors of the major components of the disorder refine to 0.721(6) and 0.858(6). The H atoms for O3W' could not be retrieved. Apart from the hydrogen bonds between carbonyl and water molecules, there are specified hydrogen bonds between chloride ion and water molecules (hydrogen bond details are provided in Appendix V Table AV.3).

Compound [Ni(**L2**)]PF_6*:* The structure is partly disordered. The PF_6^- counter ion is found to be disordered over two orientations, and the occupancy factor of the major component of the disorder refines to 0.869(9).

5.4.4 Ligand and complex synthesis

H_2**L1**Cl:
N-pyridin-2-ylmethylimidazole (6 mmol, 0.960 g) and 2-chloro-*N*-(pyridin-2-ylmethyl)acetamide (5 mmol, 0.925 g) were added into a 100 ml round-bottomed flask containing 25 ml dry ethanol. The mixture was heated at 80 °C for 5 h, after which the solvent was removed by rotary evaporation. The residue was dissolved in THF and the solution was filtered. The filtrate was concentrated to 5 ml and acetone was added until a yellow precipitate appeared. The yellow-brownish powder was collected by filtration, washed with diethyl ether, and dried under vacuum. Yield: 0.92 g (54% based on the acetamide). ^{1}H NMR (300 MHz, DMSO-d_6) δ 9.32 (s, 1H, NC*H*N), 9.15 (t, *J* = 5.6 Hz, 1H, N*H*), 8.54 (dd, *J* = 11.4, 4.8 Hz, 2H, Py-*H*), 7.89 (td, *J* = 7.7, 1.8 Hz, 1H, Py-*H*), 7.78 (m, 3H, Py-*H*), 7.54 – 7.21 (m, 4H, Py-*H*, $C_{imidazole}$-*H*), 5.62 (s, 2H, Py-CH_2-$N_{imidazole}$), 5.17 (s, 2H, Py-CH_2-N_{Amide}), 4.44 (d, *J* = 5.8 Hz, 2H, C(O)-CH_2-$N_{imidazole}$). ^{13}C NMR (75 MHz, DMSO-d_6) δ = 165.13, 157.60, 153.57, 149.61, 148.94, 137.54, 136.79, 123.96, 123.68,

122.59, 122.49, 122.35, 121.32, 53.05, 50.65, 44.42. The signal of N-*C*H-N could not be found. ESI-MS found (calc): $[M–Cl]^+$ *m/z* 308.2 (308.15).

H_2**L2**Cl:
The same synthetic procedure of H**L1**Cl was followed, but with the starting material *N*-pyridin-2-ylmethylbenzimidazole (8.5 mmol, 1.78 g) and 2-chloro-*N*-(pyridin-2-ylmethyl)acetamide (8.5 mmol, 1.6 g) in 25 ml dry ethanol at 80 °C for 60 h. Yield: 0.90 g (30% based on the acetamide). ^{1}H NMR (300 MHz, DMSO-d_6) δ 10.02 (s, 1H, NC*H*N), 9.44 (s, 1H, N*H*), 8.56 (d, *J* = 4.7 Hz, 1H, Py-*H*), 8.49 (d, *J* = 4.6 Hz, 1H, Py-*H*), 8.02 (d, *J* = 7.1 Hz, 1H, Py-*H*), 7.98 – 7.81 (m, 3H, Py-*H*), 7.73 – 7.59 (m, 3H, Py-*H*, C_{benzim}-*H*), 7.46 (d, *J* = 7.8 Hz, 1H, C_{benzim}-*H*), 7.37 (q, *J* = 7.7 Hz, 2H, C_{benzim}-*H*), 5.99 (s, 2H, Py-CH_2-N_{benzim}), 5.55 (s, 2H, Py-CH_2-N_{Amide}), 4.51 (s, 2H, C(O)-CH_2-N_{benzim}). ^{13}C NMR (75 MHz, DMSO-d_6) δ = 165.07, 152.99, 149.67, 148.29, 144.16, 137.63, 131.65, 130.95, 126.76, 123.79, 122.81, 122.70, 121.71, 113.91, 50.92, 48.66, 44.14. ESI-MS found (calc): $[M–Cl]^+$ *m/z* 358.2 (358.17).

[Ni(**L1**)]Cl:
A Schlenk flask was charged with [Ni(dme)Cl_2] (0.5 mmol, 0.11 g), H_2**L1**Cl (0.5 mmol, 0.17 g), K_2CO_3 (1.9 mmol, 0.26 g) and dry DMF (10 mL) under an argon atmosphere. The dark green solution was stirred at room temperature overnight. The reaction mixture was filtered to remove the salts. To the solution 100 ml distilled water was added and the aqueous solution was washed with DCM (3×50 ml). The water layer was evaporated to dryness. The resulting yellow solid was collected and dried under vacuum. Crystals suitable for X-ray diffraction were obtained by vapor diffusion of diethyl ether into an acetonitrile solution of the complex. Yield: 28% (56 mg). ^{1}H NMR (300 MHz, DMSO-d_6) δ 9.09 (d, *J* = 5.5 Hz, 1H, Py-H), 8.22 (t, *J* = 7.1 Hz, 1H, Py-H), 8.10 (t, *J* = 7.3 Hz, 1H, Py-H), 7.86 (d, *J* = 7.6 Hz, 1H, Py-H), 7.70 (m, 3H, Py-H), 7.49 (d, *J* = 8.6 Hz, 3H, Py-H, NCH), 5.74 (s, 2H, Py-CH_2-N_{NHC}), 4.74 (s, 2H, Py-CH_2-N_{Amide}), 4.71 (broad, 2H, C_{Amide}-CH_2-N_{NHC}). ^{13}C NMR (75 MHz, DMSO-d_6) δ = 214.87, 168.08, 163.85, 154.40, 153.52, 149.09, 147.32, 140.51, 139.53, 125.64, 123.37, 122.38, 122.08, 121.19, 58.04, 52.27, 51.92. Anal. Calcd for $C_{17}H_{16}ClN_5NiO{\cdot}1.5H_2O$: C 47.76, H 4.48, N 16.38; found C 47.58, H 4.78, N 16.25. ESI-MS found (calc): $[M–Cl]^+$ *m/z* 364.1 (364.07).

[Ni(**L2**)]PF_6:
A Schlenk flask was charged with [Ni(dme)Cl_2] (0.5 mmol, 0.11 g), H_2**L2**Cl (0.5 mmol, 0.195 g), NH_4PF_6 (0.5 mmol, 0.10 g), K_2CO_3 (1.9 mmol, 0.26 g) and dry DMF (10 mL) under an argon atmosphere. The brown solution was stirred at room temperature for 2 days. The reaction mixture was filtered and the filtrate was left standing for a few days, during which time yellow crystals formed. The crystalline solid was collected by filtration, washed with diethyl ether and dried under vacuum. Yield: 22% (60 mg). Yellow needle crystals suitable for X -ray crystallography crystals were obtained directly from filtrate after the reaction. The compound is poorly soluble in DMSO. ^{1}H NMR (400 MHz, acetonitrile-d_3) δ 8.93 (d, *J* = 5.6 Hz, 2H, Py-H), 8.12 (t, *J* = 7.7 Hz, 1H, Py-H), 8.01 (t, *J* = 7.7 Hz, 1H, Py-

H), 7.80 (dd, J = 16.2, 7.9 Hz, 2H, NCH), 7.62 (m, 3H, Py-H), 7.48 (m, 3H, Py-H, Ar-H), 7.34 (t, J = 6.6 Hz, 1H, Ar-H), 5.79 (s, 2H, Py-CH_2-N_{NHC}), 4.89 (s, 2H, Py-CH_2-N_{Amide}), 4.82 (broad, 2H, C_{Amide}-CH_2-N_{NHC}). ^{13}C NMR (101 MHz, acetonitrile-d_3) δ = 154.40, 148.69, 141.76, 140.89, 127.05, 126.88, 125.33, 125.26, 124.41, 122.32, 112.35, 111.93, 59.50, 50.85, 50.52. The six quaternary carbons could not be detected due to the low concentration caused by the limited solubility of the compound. Anal. Calcd for $C_{21}H_{18}F_6N_5NiOP$: C 45.03, H 3.24, N 12.50; found C 44.26, H 3.42, N 12.07. ESI-MS found (calc): $[M–PF_6]^+$ *m/z* 414.1 (414.09).

5.5 Acknowledgements

S. Luo gratefully acknowledges a grant from the Chinese Scholarship Council (no. 201306410011). We thank Mr. J.M.M. van Brussel for ESI-MS measurements.

5.6 References

[1] B. Rausch, M.D. Symes, G. Chisholm, L. Cronin, *Science* 2014, 345, 1326-1330.
[2] T.R. Simmons, G. Berggren, M. Bacchi, M. Fontecave, V. Artero, *Coord. Chem. Rev.* 2014, 270, 127-150.
[3] N. Kaeffer, A. Morozan, J. Fize, E. Martinez, L. Guetaz, V. Artero, *ACS Catalysis* 2016, 6, 3727-3737.
[4] E.S. Rountree, D.J. Martin, B.D. McCarthy, J.L. Dempsey, *ACS Catalysis* 2016, 3326-3335.
[5] D.L. DuBois, R.M. Bullock, *Eur. J. Inorg. Chem.* 2011, 1017-1027.
[6] J.P. Porcher, T. Fogeron, M. Gomez-Mingot, E. Derat, L.M. Chamoreau, Y. Li, M. Fontecave, *Angew. Chem. Int. Ed.* 2015, 54, 14090-14093.
[7] X.W. Song, X.J. Gao, H.X. Liu, H. Chen, C.N. Chen, *Inorg. Chem. Commun.* 2016, 70, 1-3.
[8] K. Hou, H.T. Poh, W.Y. Fan, *Chem. Commun.* 2014, 50, 6630-6632.
[9] P. Zhang, M. Wang, Y. Yang, T. Yao, L. Sun, *Angew. Chem. Int. Ed.* 2014, 53, 13803-13807.
[10] J. Berding, M. Lutz, A.L. Spek, E. Bouwman, *Organometallics* 2009, 28, 1845-1854.
[11] J. Berding, T.F. van Dijkman, M. Lutz, A.L. Spek, E. Bouwman, *Dalton Trans.* 2009, 6948-6955.
[12] Z. Xi, B. Liu, W. Chen, *J. Org. Chem.* 2008, 73, 3954-3957.
[13] M.C. Jahnke, T. Pape, F.E. Hahn, *Eur. J. Inorg. Chem.* 2009, 1960-1969.
[14] K. Kawano, K. Yamauchi, K. Sakai, *Chem. Commun.* 2014, 50, 9872-9875.
[15] M. van der Meer, E. Glais, I. Siewert, B. Sarkar, *Angew. Chem. Int. Ed.* 2015, 54, 13792-13795.
[16] M.H. Reineke, M.D. Sampson, A.L. Rheingold, C.P. Kubiak, *Inorg. Chem.* 2015, 54, 3211-3217.
[17] P. Comba, W. Goll, B. Nuber, K. Várnagy, *Eur. J. Inorg. Chem.* 1998, 2041-2049.
[18] N.W. Alcock, G. Clarkson, P.B. Glover, G.A. Lawrance, P. Moore, M. Napitupulu, *Dalton Trans.* 2005, 518-527.
[19] F.A. Chavez, M.M. Olmstead, P.K. Mascharak, *Inorg. Chem.* 1996, 35, 1410-1412.

[20] V. Fourmond, S. Canaguier, B. Golly, M.J. Field, M. Fontecave, V. Artero, *Energy Environ Sci.* 2011, 4, 2417-2427.
[21] R.S. Nicholson, I. Shain, *Anal. Chem.* 1964, 36, 706-723.
[22] M.P. Stewart, M.-H. Ho, S. Wiese, M.L. Lindstrom, C.E. Thogerson, S. Raugei, R.M. Bullock, M.L. Helm, *J. Am. Chem. Soc.* 2013, 135, 6033-6046.
[23] E.S. Rountree, B.D. McCarthy, T.T. Eisenhart, J.L. Dempsey, *Inorg. Chem.* 2014, 53, 9983-10002.
[24] L. Gan, T.L. Groy, P. Tarakeshwar, S.K.S. Mazinani, J. Shearer, V. Mujica, A.K. Jones, *J. Am. Chem. Soc.* 2015, 137, 1109-1115.
[25] R. Tatematsu, T. Inomata, T. Ozawa, H. Masuda, *Angew. Chem. Int. Ed.* 2016, 55, 5247-5250.
[26] E.I. Musina, V.V. Khrizanforova, I.D. Strelnik, M.I. Valitov, Y.S. Spiridonova, D.B. Krivolapov, I.A. Litvinov, M.K. Kadirov, P. Lonnecke, E. Hey-Hawkins, Y.H. Budnikova, A.A. Karasik, O.G. Sinyashin, *Chem. -Eur. J.* 2014, 20, 3169-3182.
[27] R.M. Stolley, J.M. Darmon, M.L. Helm, *Chem. Commun.* 2014, 50, 3681-3684.
[28] V. Fourmond, P.-A. Jacques, M. Fontecave, V. Artero, *Inorg. Chem.* 2010, 49, 10338-10347.
[29] P.F. Huo, C. Uyeda, J.D. Goodpaster, J.C. Peters, T.F. Miller, *ACS Catalysis* 2016, 6, 6114-6123.
[30] A. Kermagoret, P. Braunstein, *Organometallics* 2008, 27, 88-99.
[31] M. Woods, A.D. Sherry, *Inorg. Chem.* 2003, 42, 4401-4408.
[32] J. Dinda, S.D. Adhikary, S.K. Seth, A. Mahapatra, *New J. Chem.* 2013, 37, 431-438.
[33] G.M. Sheldrick, *Acta Cryst. C* 2015, 71, 3-8.